PH3 revisited: Theoretical transition moments for the vibrational transitions below

ARTICLE *in* JOURNAL OF MOLECULAR SPECTROSCOPY · DECEMBER 2008

Impact Factor: 1.48 · DOI: 10.1016/j.jms.2008.07.005

Journal of Molecular Spectroscopy 252 (2008) 121–128

Contents lists available at ScienceDirect

Journal of Molecular Spectroscopy

journal homepage: www.elsevier.com/locate/jms

PH_3 revisited: Theoretical transition moments for the vibrational transitions below 7000 cm^{-1}

Roman I. Ovsyannikov [a,1], Walter Thiel [b], Sergei N. Yurchenko [c], Miguel Carvajal [d], Per Jensen [a,*]

[a] Theoretische Chemie, Bergische Universität, D-42097 Wuppertal, Germany
[b] Max-Planck-Institut für Kohlenforschung, Kaiser-Wilhelm-Platz 1, D-45470 Mülheim an der Ruhr, Germany
[c] Technische Universität Dresden, Institut für Physikalische Chemie und Elektrochemie, D-01062 Dresden, Germany
[d] Departamento de Física Aplicada, Facultad de Ciencias Experimentales, Avenida de las Fuerzas Armadas s/n, Universidad de Huelva, E-21071 Huelva, Spain

ARTICLE INFO

Article history:
Received 29 June 2008
Available online 25 July 2008

Keywords:
PH_3
Phosphine
Ab initio
Variational calculations
Vibrational spectra
Transition moments
Local modes

ABSTRACT

We present here an extensive list of theoretical vibrational transition moments for the electronic ground state of PH_3, covering all transitions with significant intensities in the wavenumber region below 7000 cm^{-1}. This work complements, and uses a potential energy surface from, our recent calculation of vibrational term values for PH_3 [R.I. Ovsyannikov, W. Thiel, S.N. Yurchenko, M. Carvajal, P. Jensen, J. Chem. Phys. 129 (2008) 044309] and it extends, and uses a dipole moment surface from, our previous work on PH_3 intensities [S.N. Yurchenko, M. Carvajal, W. Thiel, P. Jensen, J. Mol. Spectrosc. 239 (2006) 71–87]. Owing to an improved potential energy surface, the transition-moment results of the present work constitute a significant improvement over our previous work. The quality of the reproduction of the available experimental data suggests that we are approaching a situation where theoretical calculations of intensity information can compete with, and possibly in some cases replace, experimental determinations of intensities for small molecules. We demonstrate that the theoretical intensity results of the present work are in accordance with the predictions of local-mode theory.

1. Introduction

In a very recent publication [1], we have reported the calculation of a new *ab initio* potential energy surface (PES) for the electronic ground state of PH_3. The surface was obtained at the CCSD(T) level of theory, using aug-cc-pV(Q+d)Z and aug-cc-pVQZ basis sets for P and H, respectively, and including scalar relativistic corrections. The computed *ab initio* energies were used to construct an analytical, parameterized representation of the PES, and (after an empirical adjustment of one parameter, the equilibrium value of the bond angle) the resulting parameter values served as input for calculations of vibrational energies for PH_3 carried out by means of the newly developed program TROVE (Theoretical ROVibrational Energies) [2]. The CVBS (Complete Vibrational Basis Set) extrapolation scheme [1], analogous to the CBS (Complete Basis Set) limit schemes [3,4] used in electronic structure calculations, was employed to improve the convergence of the TROVE-calculated vibrational energies with increasing vibrational basis-set size. The CVBS-extrapolated values for the vibrational energies of PH_3 were found to be in excellent agreement with the available, experimentally derived term values.

The work reported in Ref. [1] extends our previous studies of PH_3 [5–7], in which we applied the program XY3 [8,9] to the calculation of rotation–vibration energies and intensities. Initially [5], we refined an *ab initio* PES from Wang et al. [10] in a simultaneous least-squares fitting to *ab initio* data and experimentally derived vibrational energy spacings, and we used the refined PES to determine vibrational term values of PH_3. The calculation of energies for highly excited rotational states was the subject of Ref. [6] where we showed theoretically that for PH_3, such states form sixfold near-degenerate energy clusters analogous to the fourfold energy clusters in H_2X molecules [11,12]. Apart from Ref. [1], the most recent addition to the PH_3 work is a calculation [7] of the transition moments for vibrational bands and the intensities for individual rotation–vibration transitions; these computations put special emphasis on transitions involving the cluster states described in Ref. [6].

In Ref. [7] we reported vibrational transition moments for selected vibrational transitions of PH_3, calculated with the XY3 program [8,9] from a refined version (the refinements carried out as described in Ref. [5]) of the *ab initio* PES from Ref. [10] and from

* Corresponding author. Fax: +49 202 439 2509.
E-mail address: jensen@uni-wuppertal.de (P. Jensen).
[1] On leave from: Institute of Applied Physics, Russian Academy of Science, Uljanov Street 46, Nizhnii Novgorod 603950, Russia.

0022-2852/$ - see front matter © 2008 Elsevier Inc. All rights reserved.
doi:10.1016/j.jms.2008.07.005

a dipole moment surface (DMS) calculated *ab initio* at the CCSD(T)/aug-cc-pVTZ level of theory [7] and referred to as the ATZfc DMS. In the present work, we extend the list of computed transition moments and effective intensities [see Eqs. (11) and (12) below] to comprise all vibrational transitions calculated to lie in the wavenumber interval $0-7000\ \mathrm{cm}^{-1}$ and to have significant intensity at an absolute temperature of 300 K. The vibrational transition-moment calculations of the present work are carried out with the AV(Q+d)Z+R PES (see Section 2 for the notation) obtained in Ref. [1] and the ATZfc DMS from Ref. [7]. The resulting vibrational transition moments reproduce the available experimental values significantly better than those from Ref. [7]. We also give here an analysis, in terms of local-mode theory [13,14], of the computed vibrational transition moments. It is shown that the theoretical results are in keeping with the predictions of local-mode theory.

2. The *ab initio* calculation

We have already explained in Ref. [1] how we have used the MOLPRO2002 program [15,16] to calculate the PES for the electronic ground state of PH_3 by means of the CCSD(T) method (i.e., coupled cluster theory with all single and double substitutions [17] and a perturbative treatment of connected triple excitations [18,19]). In these calculations, we employed Dunning basis sets [20–23]: aug-cc-pV(Q+d)Z and aug-cc-pVQZ for P and H, respectively. We label the resulting *ab initio* data points, and their analytical representation (see below), as AV(Q+d)Z. The energies were subsequently corrected by the mass–velocity and the one-electron Darwin terms, computed at the CCSD(T) level with the aug-cc-pV(T+d)Z (for P) and aug-cc-pVTZ (for H) basis sets. The resulting PES, which includes relativistic effects, is referred to as AV(Q+d)Z+.

The AV(Q+d)Z and AV(Q+d)Z+ *ab initio* points were fitted in terms of the analytical function given in Eqs. (1)–(7) of Ref. [1]. This function is discussed in general in Ref. [8], where it is called a PES-type-A. It is essentially an expansion in the stretching and bending coordinates

$$\xi_k = 1 - \exp(-a(r_k - r_e)), \quad k = 1,2,3, \tag{1}$$

$$\xi_{4a} = \frac{1}{\sqrt{6}}(2\alpha_{23} - \alpha_{13} - \alpha_{12}), \tag{2}$$

$$\xi_{4b} = \frac{1}{\sqrt{2}}(\alpha_{13} - \alpha_{12}), \tag{3}$$

and

$$\sin\bar{\rho} = \frac{2}{\sqrt{3}}\sin[(\alpha_{12} + \alpha_{13} + \alpha_{23})/6] \tag{4}$$

for the 'umbrella' motion. In Eqs. (1)–(4), a is a molecular parameter, the bond length $r_i (i = 1,2,3)$ is defined as the instantaneous distance between the P nucleus and proton i (where the protons of the PH_3 molecule are labeled as 1, 2, and 3, respectively, and the P nucleus as 4), and the bond angle $\alpha_{ij} = \angle(H_i - P - H_j)$, where H_i and H_j are the protons labeled i and j, respectively. The optimized PES-type-A parameter values for the AV(Q+d)Z+ PES are given in Table I of Ref. [1], and those for the AV(Q+d)Z PES are available from the authors on request.

As explained in Ref. [1], we realized that relative to the AV(Q+d)Z+ *ab initio* PES, we could obtain a significant improvement of the reproduction of the vibrational energies by empirically adjusting, in a least-squares fitting to experimentally derived vibrational energies, the one parameter α_e (i.e., the equilibrium bond angle value) of the analytical representation of the AV(Q+d)Z+ PES. The least-squares fitting was carried out with the TROVE program. The AV(Q+d)Z+ PES has $\alpha_e = 93.4926^\circ$ and the empirical adjustment changed this value to 93.565°; the adjusted value is very close to the original AV(Q+d)Z value of 93.556°. The resulting, adjusted PES is denoted by AV(Q+d)Z+R and the theoretical vibrational energies reported in Ref. [1] were computed with this PES.

In Table 1 we report AV(Q+d)Z and AV(Q+d)Z+ *ab initio* values of the equilibrium bond length r_e, the equilibrium bond angle α_e, and the harmonic vibrational wavenumbers ω_i for the electronic ground state of PH_3. For comparison, we also include in the table the CCSD(T)/cc-pwCVQZ values from Ref. [10] together with CCSD(T)/aug-cc-pV(5+d)Z values from the present work. The ω-values for the stretching modes ν_1 and ν_3 change the most when the basis set is extended from cc-pwCVQZ [10] to aug-cc-pV(Q+d)Z. We attribute this change to the d-functions localized at the P nucleus. It is seen that relative to the AV(Q+d)Z results, the relativistic corrections in the AV(Q+d)Z+ calculation cause some change of the equilibrium structure and the ω-values, whereas the extension of the basis set to aug-cc-pV(5+d)Z causes a much smaller change.

3. Theoretical vibrational term values calculated with TROVE

3.1. Implementation of symmetrized vibrational basis functions

The TROVE program [2] calculates the rotation–vibration energies as the eigenvalues of matrix blocks obtained by constructing the matrix representation of the rotation–vibration Hamiltonian in terms of suitable basis functions. Initially, the matrix representation is set up in terms of primitive basis functions [2]

$$\psi_n = |n_1\rangle|n_2\rangle|n_3\rangle|n_4\rangle|n_5\rangle|n_6\rangle. \tag{5}$$

Each vibrational 'factor function' $|n_i\rangle$ in Eq. (5) (with principal quantum number n_i) is a one-dimensional (1D) function $\phi_i(\xi_i^\ell)$ depending on one, and only one, of the six coordinates ξ_i^ℓ $(i = 1,\ldots,6)$ which are linearized versions [8] of the coordinates $(r_1, r_2, r_3, \alpha_{12}, \alpha_{13}, \alpha_{23})$ introduced in connection with Eqs. (1)–(4). The $\phi_i(\xi_i^\ell)$ functions are generated in numerical solutions of the corresponding 1D Schrödinger equations (for details, see Ref. [2]). In the present TROVE calculations, we use a Hamiltonian defined in terms of a rigid reference configuration, i.e., both the kinetic energy operator and the potential energy function are expressed as expansions (of 4th and 8th order, respectively) around the equilibrium geometry in the coordinates ξ_i^ℓ $(i = 1,\ldots,6)$.

In TROVE calculations for PH_3, we control the size of the vibrational basis set by a single parameter P_{max}. That is, we include in the basis set only those functions ψ_n from Eq. (5) for which $P \leqslant P_{max}$, where the polyad number P is given by [2]

$$P = 2(n_1 + n_2 + n_3) + n_4 + n_5 + n_6. \tag{6}$$

Table 1
Equilibrium geometry and harmonic vibrational wavenumbers for the electronic ground state of PH_3

Parameter	AV(Q+d)Z[a]	AV(Q+d)Z+[b]	AV(5+d)Z[c]	Ref. [10][d]	Exp.[e]
r_e/Å	1.41514	1.41473	1.41473	1.41105	1.412
α_e/°	93.5562	93.4926	93.5579	93.497	93.4
$\omega_1/\mathrm{cm}^{-1}$	2421.46	2419.12	2421.37	2429.75	
$\omega_2/\mathrm{cm}^{-1}$	1012.63	1013.83	1011.65	1016.47	
$\omega_3/\mathrm{cm}^{-1}$	2429.08	2426.76	2429.18	2437.58	
$\omega_4/\mathrm{cm}^{-1}$	1142.77	1143.41	1142.69	1147.35	

[a] From CCSD(T)/aug-cc-pV(Q+d)Z *ab initio* calculations [1].
[b] From CCSD(T)/aug-cc-pV(Q+d)Z *ab initio* calculations with relativistic corrections included [1].
[c] From CCSD(T)/aug-cc-pV(5+d)Z *ab initio* calculations (present work).
[d] CCSD(T)/cc-pwCVQZ *ab initio* results from Ref. [10].
[e] Experimentally derived values from Refs. [24,25].

The appropriate Molecular Symmetry (MS) group [12] for PH_3 is

$$\boldsymbol{C}_{3v}(M) = \{E, (123), (132), (12)^*, (23)^*, (13)^*\}, \quad (7)$$

where, for example, (123) is a cyclic permutation that causes nucleus 1 to be replaced by nucleus 2, nucleus 2 to be replaced by nucleus 3, and nucleus 3 to be replaced by nucleus 1. The operation $(12)^*$ interchanges the protons 1 and 2 and inverts all particles, nuclei and electrons, in the molecular center of mass. The general notation for permutation–inversion operations is explained in Refs. [12,26]. Table 2 gives the irreducible representations [12,26] of $\boldsymbol{C}_{3v}$(M).

A matrix representation of the vibrational Hamiltonian, constructed in terms of the primitive basis functions ψ_n from Eq. (5), is not block-diagonal. However, by 'symmetrizing' the ψ_n functions [i.e., by transforming them to functions that transform according to the irreducible representations [12,26] of $\boldsymbol{C}_{3v}$(M)] we can reduce the Hamiltonian matrix to block-diagonal form with one block for each irreducible representation of $\boldsymbol{C}_{3v}$(M). We have implemented in the TROVE program the projection-operator technique described, for example, in Ref. [12] to obtain symmetrized basis functions and the Hamiltonian matrix representation, constructed in terms of these functions, has the desired block-diagonal form with (Table 2) an A_1 block, an A_2 block, and two E-blocks with identical eigenvalues.

As described in Ref. [2], TROVE calculations can be carried out with many different choices for the 1D basis functions $|n_i\rangle$. The detailed form of these functions is not important for the symmetrization, however it is important that the three 1D stretching functions $|n_1\rangle$, $|n_2\rangle$, and $|n_3\rangle$ be symmetrically equivalent, i.e., that the operations in $\boldsymbol{C}_{3v}$(M) all have the effect of permuting them, and that $|n_4\rangle$, $|n_5\rangle$, and $|n_6\rangle$ are symmetrically equivalent in the same sense. Then, for an arbitrary set of quantum numbers $n_1 \leqslant n_2 \leqslant n_3$, $n_4 \leqslant n_5 \leqslant n_6$, we can form symmetrized linear combinations of, on one hand, $|n_1\rangle$, $|n_2\rangle$, and $|n_3\rangle$ and, on the other hand, $|n_4\rangle$, $|n_5\rangle$, and $|n_6\rangle$. In both cases, the symmetrized functions can be obtained from the results of Ref. [27]. By means of the techniques described in Ref. [12], the symmetrized stretching basis functions are finally combined with symmetrized bending basis functions to give the symmetrized vibrational basis functions.

3.2. CVBS extrapolation

To compute accurate vibrational energies we should, in principle, increase the vibrational basis set gradually by increasing the parameter P_{max} [see the discussion of Eq. (6)] until the energies of interest are converged in that they do not change appreciably upon a further increase of P_{max}. We observed in Ref. [1] that even for a very large basis set with $P_{max} = 16$, some energies associated with excited states of the 'umbrella' mode ν_2 were not fully converged. We improved the convergence of these levels by implementing the so-called CVBS limit extrapolation scheme which is analogous to the CBS limit schemes [3,4] used in electronic structure calculations. The basic idea is to do TROVE calculations for several values of P_{max} and then fit the set of energy values obtained for a given molecular state in terms of the expression

Table 2
The character table of the $\boldsymbol{C}_{3v}$ (M) group [12]

	E	(123) (132)	$(12)^*$ $(23)^*$ $(13)^*$
A_1	1	1	1
A_2	1	1	−1
E	2	−1	0

$$E_i(P_{max}) = E_i^{\infty} + a_i \exp(-P_{max}\lambda_i), \quad (8)$$

where E_i^{∞}, a_i, and λ_i are fitting parameters, and i is a short-hand notation for the vibrational quantum numbers $(\nu_1, \nu_2, \nu_3^{l_3}, \nu_4^{l_4})$ which are the customary spectroscopic labels based on an uncoupled-harmonic-oscillator approximation of the vibrational eigenfunction. The limiting value $\lim_{P_{max}\to\infty} E_i(P_{max}) = E_i^{\infty}$, and so E_i^{∞} is the CVBS-extrapolated value. We have explained in Ref. [1] how in practice, we must make separate fittings of energy values obtained with odd and even P_{max}-values, respectively. The two fittings produce a common value for the extrapolated energy E_i^{∞}.

3.3. Computed vibrational term values

With the PESs AV(Q+d)Z, AV(Q+d)Z+, and AV(Q+d)Z+R we have carried out TROVE calculations of the vibrational energies of PH_3. For each PES, we made a series of calculations with P_{max} varying from 8 through 16. The vibrational energies obtained were then extrapolated to the CVBS limit as explained in Section 3.2. The extrapolated energies are given in Table 3. The AV(Q+d)Z+R results have already been reported in Ref. [1] but we include them here for completeness.

Table 3 documents the discussion of Ref. [1] and Section 2: relative to the AV(Q+d)Z calculation, the correction of the *ab initio* data by the mass–velocity and the one-electron Darwin terms (i.e., the AV(Q+d)Z+ calculation) does not lead to a uniformly better agreement with experiment for the vibrational term values. For some term values, there is indeed an improvement, but for others, especially those of the states ν_2 $\nu_2(\nu_2 = 1, 2, 3, 4)$, where ν_2 is the 'umbrella' vibration, there is a significant deterioration. As already mentioned in Section 2 we were able to remedy this situation by empirically adjusting α_e, the equilibrium bond angle value, thus obtaining the AV(Q+d)Z+R PES. It would seem that by introducing the relativistic corrections (that is, the mass–velocity and the one-electron Darwin terms) we improved the shape of the PES while deteriorating the agreement of α_e with its experimental value. However, we suspect that this apparent success of the relativistic corrections is rather fortuitous for PH_3. It can be seen from Table 1 that an extension of the basis set from aug-cc-pV(Q+d)Z to aug-cc-pV(5+d)Z does not produce any major effects. This extension causes ω_1 to decrease slightly, which will tend to improve the agreement with experiment since the aug-cc-pV(Q+d)Z value for ν_1 is too high (Table 3). However, ω_2, ω_3, and ω_4 all change so as to cause a very slight deterioration of the agreement with experiment.

4. Electric-dipole transition moments

As already mentioned in Section 1, we have previously reported [7] transition moments for selected vibrational transitions of PH_3. We now complement the theoretical term values given in Section 3 and Ref. [1] by theoretical transition-moment values for all vibrational transitions below 7000 cm^{-1} that have a sizeable intensity at an absolute temperature of 300 K.

We have used the AV(Q+d)Z+R PES, together with the ATZfc DMS reported for PH_3 in Ref. [7], to compute the vibrational transition moments defined as

$$\mu_{fi} = \sqrt{\sum_{\alpha=x,y,z} |\langle \Phi_{vib}^{(f)} | \bar{\mu}_\alpha | \Phi_{vib}^{(i)} \rangle|^2}, \quad (9)$$

where $|\Phi_{vib}^{(w)}\rangle$, $w = i$ or f, are vibrational wavefunctions ($J = 0$), and $\bar{\mu}_\alpha$ is the component of the electronically averaged dipole moment vector [9,12] $\bar{\boldsymbol{\mu}}$ along the molecule-fixed $\alpha(= x, y, z)$ axis.

Table 3
Vibrational term values calculated with different potential energy surfaces (in cm^{-1}) of PH_3 compared to the corresponding experimental values

State[a]	I[b]	Obs.[c]	AV(Q+d)Z	Δ[d]	AV(Q+d)Z+	Δ[e]	AV(Q+d)Z+R[f]	Δ[g]
v_2	A_1	992.13	991.37	0.76	993.37	−1.23	991.90	0.23
$2v_2$	A_1	1972.57[h]	1971.60	0.97	1975.42	−2.85	1972.38	0.19
$2v_4^0$	A_1	2226.83[i]	2224.70	2.13	2226.87	−0.03	2227.73	−0.90
v_1	A_1	2321.12[i]	2323.17	−2.05	2321.15	−0.03	2321.04	0.08
$3v_2$	A_1	2940.77	2940.48	0.29	2945.96	−5.20	2941.07	−0.30
$v_2 + 2v_4^0$	A_1	3214.2	3209.41	5.52	3213.23	1.71	3212.57	2.36
$v_1 + v_2$	A_1	3305.8	3308.39	−0.83	3308.49	−0.93	3306.88	0.68
$4v_2$	A_1	3896.02	3897.86	−1.84	3904.86	−8.84	3897.14	−1.12
$v_1 + 2v_2$	A_1	4282.4	4282.05	0.35	4284.10	−1.70	4280.79	1.61
$2v_1$	A_1	4566.26	4567.15	−0.89	4563.81	2.45	4563.72	2.54
$2v_3$	A_1	4644.66	4647.60	−2.94	4643.81	0.85	4643.68	0.98
$2v_1 + 2v_2$	A_1	6503.1	6511.14	−8.04	6505.00	−1.90	6503.86	−0.76
$3v_1$	A_1	6714.60	6712.78	1.82	6709.41	5.19	6715.32	−0.72
$v_1 + 2v_3$	A_1	6881.53	6885.82	−4.29	6880.17	1.36	6879.90	1.63
$3v_3^3$	A_1	6971.16	6974.03	−2.87	6968.79	2.37	6968.65	2.51
v_4	E	1118.31	1117.43	0.88	1118.50	−0.20	1118.93	−0.63
$v_2 + v_4$	E	2108.15[i]	2106.07	2.08	2108.97	−0.82	2107.93	0.22
$2v_4^2$	E	2234.93[i]	2233.08	1.84	2235.26	−0.34	2236.11	−1.19
v_3	E	2326.87[i]	2327.43	−0.56	2325.78	1.09	2325.80	1.06
$2v_2 + v_4$	E	3085.65[h]	3082.54	3.12	3087.06	−1.41	3084.35	1.30
$v_1 + v_4$	E	3423.9	3425.76	−1.86	3425.11	−1.21	3425.48	−1.58
$v_1 + v_3$	E	4565.78	4567.47	−1.69	4564.11	1.67	4564.02	1.76
$v_2 + 2v_3^2$	E	5540.0	5544.64	−4.64	5543.50	−3.50	5541.73	−1.73
$2v_1 + v_4$	E	5645.4	5653.01	−7.61	5642.26	3.14	5643.12	2.28
$3v_2^1$	E	6714.6	6712.12	2.48	6708.03	6.57	6711.56	3.04
$2v_1 + v_3$	E	6883.73	6888.01	−4.28	6882.62	1.11	6882.31	1.42
$v_1 + 2v_3^2$	E	6890.86	6892.34	−1.48	6887.41	3.45	6887.20	3.66

[a] Spectroscopic assignment of the vibrational band.
[b] Symmetry of the vibrational state in $\boldsymbol{C}_{3v}(M)$.
[c] See Ref. [10] for original references unless otherwise indicated.
[d] E(Obs.) − E(AV(Q+d)Z) in cm^{-1}.
[e] E(Obs.) − E(AV(Q+d)Z+) in cm^{-1}.
[f] From Ref. [1].
[g] E(Obs.) − E(AV(Q+d)Z+R) in cm^{-1}.
[h] From Ref. [28].
[i] From Ref. [29].

Table 4
Vibrational band centers $\tilde{\nu}_{fi}$ and transition-moment values μ_{fi} for transitions originating in the vibrational ground state

Band[a]	$\tilde{\nu}_{fi}$ (cm^{-1})		μ_{fi}(D)		
	Obs.[b]	Present work	Obs.[b]	Ref. [7]	Present work
g.s.			0.57395	0.5832	0.58533
v_2	992.13	991.90	0.08251	0.0846	0.0845
$2v_2$	1972.57	1972.38	0.00299	0.0027	0.0022
$2v_4^0$	2226.83	2227.73	0.0176	0.0055	0.0173
v_1	2321.12	2321.04	0.069	0.0732	0.0696
v_4	1118.31	1118.93	0.08626	0.0865	0.0882
$v_2 + v_4$	2108.15	2107.93	0.01102	0.0093	0.0087
$2v_4^2$	2234.93	2236.11	0.0176	0.0015	0.0136
v_3	2326.87	2325.80	0.13	0.1389	0.1379

[a] Spectroscopic assignment for the upper vibrational state.
[b] See Ref. [7] for original references.

The matrix elements required are generated with the computer program XY3 [8,9]. The technical details of the computation procedure can be found in Ref. [7]. The XY3 program employs the same vibrational basis set as TROVE [see Eq. (5)] and the size of the basis set used in the XY3 calculations was determined by setting $P_{max} = 14$ in Eq. (6). Analogous calculations have already been carried out for NH_3 [30] and NH_3^+ [31].

Table 4 lists the vibrational transitions originating in the vibrational ground state, for which the transition moment has been experimentally determined. The experimentally derived transition-moment values $(\mu_{fi})^{(obs)}$ are compared with theoretical values $(\mu_{fi})^{(calc)}$ from Ref. [7] and from the present work. The transition-moment values from Ref. [7] are calculated with a refined version of the *ab initio* PES from Wang et al. [10] and with the ATZfc DMS from Ref. [7]. The vibrational term values included in the table are calculated from the AV(Q+d)Z+R PES with TROVE in conjunction with CVBS extrapolation.

The relative root-mean-square deviation between the $(\mu_{fi})^{(obs)}$ and $(\mu_{fi})^{(calc)}$ values in Table 4 is defined as

$$\sigma_{rel} = \sqrt{\frac{1}{N_{val}} \sum_{k=1}^{N_{val}} \left(\frac{(\mu_{fi})_k^{(obs)} - (\mu_{fi})_k^{(calc)}}{(\mu_{fi})_k^{(obs)}} \right)^2}, \quad (10)$$

where the index k numbers the transition-moment values and $N_{val} = 9$ in the present case. When we compare the theoretical transition moments from Ref. [7] with the experimental values, we calculate $\sigma_{rel} = 0.39$, whereas we get $\sigma_{rel} = 0.14$ with the theoretical transition moments from the present work. Thus, the transition-moment results of the present work constitute a significant improvement over those in Ref. [7].

In Tables 5 and 6 we report a list of transition moments for transitions from the vibrational ground state covering the wavenumber range from 0 to 7000 cm^{-1}. The vibrational term values included in the tables are calculated from the AV(Q+d)Z+R PES with TROVE in conjunction with CVBS extrapolation. We have selected transitions with substantial intensity values also at temperatures $T \leqslant 300$ K. The transition moments μ_{fi} are temperature-independent quantities. The strength of the vibrational band at a given temperature can be calculated as [32]

$$S_{vib}(f \leftarrow i) = \frac{8\pi^3 \tilde{\nu}_{fi}}{3hc} \frac{LT_0}{Q_{vib}(T)T} e^{-E_i/kT} \left[1 - e^{-(E_f - E_i)/kT}\right] \mu_{fi}^2, \quad (11)$$

where E_i and E_f are the band centers of the initial and final states, respectively, $\tilde{\nu}_{fi} = (E_f - E_i)/(hc)$, h is Planck's constant, c is the speed

Table 5
Vibrational band centers $\tilde{\nu}_{fi}$ (in cm^{-1}), transition moments μ_{fi} (in D), and vibrational band strengths S_{vib} (in cm^{-2} atm^{-1} at $T = 300$ K) for PH_3 transitions originating in the ground vibrational state

Band[a]	Γ_f[b]	$\tilde{\nu}_{fi}$	μ_{fi}	S_{vib}
g.s.	A_1	0.00	0.58533	3.4453[c]
ν_2	A_1	991.90	0.08454	71.2837
ν_4	E	1118.93	0.08816	87.4489
$2\nu_2$	A_1	1972.38	0.00219	0.0947
$\nu_2+\nu_4$	E	2107.93	0.00870	1.6058
$2\nu_4$	A_1	2227.73	0.01730	6.7036
$2\nu_4$	E	2236.11	0.01361	4.1623
ν_1	A_1	2321.04	0.06956	112.9179
ν_3	E	2325.80	0.13789	444.6091
$3\nu_2$	A_1	2941.07	0.00263	0.2052
$2\nu_2+\nu_4$	E	3084.35	0.00126	0.0489
$\nu_2+2\nu_4$	A_1	3212.57	0.00172	0.0956
$\nu_2+2\nu_4$	E	3221.19	0.00103	0.0346
$\nu_1+\nu_2$	A_1	3306.88	0.00294	0.2878
$\nu_2+\nu_3$	E	3311.22	0.00128	0.0542
$3\nu_4$	E	3333.92	0.00047	0.0073
$\nu_3+\nu_4$	A_2	3425.13	0.01014	3.5448
$\nu_3+\nu_4$	E	3436.29	0.00044	0.0067
$\nu_3+\nu_4$	A_1	3441.01	0.00504	0.8801
$2\nu_2+2\nu_4$	A_1	4182.48	0.00042	0.0073
$\nu_1+2\nu_2$	A_1	4280.79	0.00085	0.0313
$2\nu_2+\nu_3$	E	4285.64	0.00125	0.0670
$\nu_1+\nu_2+\nu_4$	E	4407.33	0.00122	0.0663
$\nu_2+\nu_3+\nu_4$	E	4419.45	0.00062	0.0172
$\nu_2+\nu_3+\nu_4$	A_1	4423.68	0.00054	0.0132
$4\nu_4$	A_1	4428.55	0.00051	0.0114
$4\nu_4$	E	4436.96	0.00034	0.0052
$\nu_3+2\nu_4$	E	4518.98	0.00179	0.1460
$\nu_1+2\nu_4$	A_1	4519.90	0.00186	0.1564
$\nu_1+2\nu_4$	E	4537.44	0.00045	0.0094
$\nu_3+2\nu_4$	E	4547.88	0.00082	0.0305
$2\nu_1$	A_1	4563.72	0.00351	0.5667
$\nu_1+\nu_3$	E	4564.02	0.00641	1.8862
$2\nu_3$	A_1	4643.68	0.00125	0.0727
$\nu_1+3\nu_2$	A_1	5242.30	0.00045	0.0107
$3\nu_2+\nu_3$	E	5248.81	0.00071	0.0268
$\nu_1+\nu_2+2\nu_4$	A_1	5496.83	0.00041	0.0092
$2\nu_1+\nu_2$	A_1	5541.52	0.00049	0.0136
$\nu_1+\nu_2+\nu_3$	E	5541.73	0.00155	0.1334
$\nu_3+3\nu_4$	A_2	5603.84	0.00087	0.0426
$\nu_2+2\nu_3$	A_1	5623.13	0.00069	0.0271
$\nu_3+3\nu_4$	E	5643.12	0.00055	0.0170
$\nu_3+3\nu_4$	E	5649.75	0.00112	0.0716
$\nu_3+3\nu_4$	E	5653.12	0.00141	0.1132
$\nu_1+\nu_3+\nu_4$	E	5673.05	0.00034	0.0067
$\nu_1+\nu_3+\nu_4$	A_1	5673.64	0.00046	0.0119
$2\nu_3+\nu_4$	E	5748.98	0.00034	0.0067
$\nu_3+4\nu_4$	A_2	6708.28	0.00027	0.0051
$\nu_1+2\nu_3$	A_1	6879.90	0.00033	0.0076

[a] Spectroscopic assignment of the vibrational band.
[b] Symmetry of the final vibrational state in $\boldsymbol{C}_{3v}(M)$.
[c] We used an effective value $\tilde{\nu}_{fi} = 1.0$ cm^{-1} instead of $\tilde{\nu}_{fi} = 0.0$ cm^{-1} in Eq. (11) in order to estimate S_{vib} for the ground-state rotational spectrum.

Table 6
Vibrational band centers $\tilde{\nu}_{fi}$ (in cm^{-1}), transition moments μ_{fi} (in D), and vibrational band strength S_{vib} (in cm^{-2} atm^{-1} at $T = 300$ K) for a number of hot $^{14}PH_3$ transitions

Band[a]	Γ_f[b]	Γ_i[c]	$\tilde{\nu}_{fi}$	μ_{fi}	S_{vib}
$2\nu_2-\nu_2$	A_1	A_1	980.48	0.11498	1.1198
$\nu_2+\nu_4-\nu_2$	E	A_1	1116.03	0.08675	0.7256
$2\nu_4-\nu_2$	A_1	A_1	1235.83	0.00736	0.0058
$\nu_1-\nu_2$	A_1	A_1	1329.14	0.00836	0.0080
$\nu_3-\nu_2$	E	A_1	1333.90	0.01275	0.0187
$2\nu_2+\nu_4-\nu_2$	E	A_1	2092.45	0.01171	0.0248
$\nu_2+2\nu_4-\nu_2$	A_1	A_1	2220.67	0.01516	0.0441
$\nu_2+2\nu_4-\nu_2$	E	A_1	2229.28	0.01264	0.0308
$\nu_1+\nu_2-\nu_2$	A_1	A_1	2314.98	0.06852	0.9390
$\nu_2+\nu_3-\nu_2$	E	A_1	2319.32	0.13523	3.6638
$3\nu_4-\nu_2$	E	A_1	2342.01	0.01009	0.0215
$\nu_3+\nu_4-\nu_2$	A_1	A_1	2449.10	0.00471	0.0047
$4\nu_2-\nu_2$	A_1	A_1	2905.24	0.00534	0.0071
$\nu_1+\nu_2+\nu_4-\nu_2$	E	A_1	3415.42	0.01031	0.0314
$\nu_2+\nu_3+\nu_4-\nu_2$	A_1	A_1	3431.77	0.00449	0.0060
$2\nu_1+\nu_2-\nu_2$	A_1	A_1	4549.61	0.00342	0.0046
$\nu_1+\nu_2+\nu_3-\nu_2$	E	A_1	4549.83	0.00677	0.0180
$\nu_4-\nu_4$	E	E	0.00	0.83704	0.0329
$\nu_2+\nu_4-\nu_4$	E	E	989.00	0.11786	0.6452
$2\nu_4-\nu_4$	A_1	E	1108.80	0.08520	0.3780
$\nu_2+2\nu_4-\nu_4$	A_1	E	2093.64	0.00853	0.0072
$3\nu_4-\nu_4$	E	E	2214.98	0.03838	0.1533
$3\nu_4-\nu_4$	A_2	E	2231.90	0.01680	0.0296
$3\nu_4-\nu_4$	A_1	E	2232.07	0.01957	0.0402
$\nu_3+\nu_4-\nu_4$	A_2	E	2306.19	0.09668	1.0123
$\nu_1+\nu_4-\nu_4$	E	E	2306.55	0.08776	0.8342
$\nu_3+\nu_4-\nu_4$	E	E	2317.36	0.06312	0.4335
$\nu_3+\nu_4-\nu_4$	A_1	E	2322.07	0.09659	1.0173
$\nu_1+\nu_2+\nu_4-\nu_4$	E	E	3288.39	0.00666	0.0069
$\nu_2+\nu_3+\nu_4-\nu_4$	E	E	3300.51	0.00552	0.0047
$\nu_3+2\nu_4-\nu_4$	E	E	3400.04	0.00980	0.0153
$\nu_1+2\nu_4-\nu_4$	E	E	3418.50	0.00719	0.0083
$\nu_3+2\nu_4-\nu_4$	E	E	3428.95	0.00648	0.0068
$\nu_1+\nu_3+\nu_4-\nu_4$	E	E	4554.11	0.00477	0.0049
$\nu_1+\nu_3+\nu_4-\nu_4$	A_1	E	4554.70	0.00484	0.0050
$3\nu_2-2\nu_2$	A_1	A_1	968.68	0.13492	0.0138
$2\nu_2+\nu_4-2\nu_2$	E	A_1	1111.97	0.08563	0.0064
$\nu_1+2\nu_2-2\nu_2$	A_1	A_1	2308.40	0.06772	0.0083
$2\nu_2+\nu_3-2\nu_2$	E	A_1	2313.26	0.13245	0.0318
$2\nu_2+\nu_4-\nu_2+\nu_4$	E	E	976.42	0.16027	0.0103
$\nu_1+\nu_2+\nu_4-(\nu_2+\nu_4)$	E	E	2299.39	0.08850	0.0074
$\nu_2+\nu_3+\nu_4-(\nu_2+\nu_4)$	A_2	E	2299.59	0.09479	0.0085
$\nu_2+\nu_3+\nu_4-(\nu_2+\nu_4)$	A_1	E	2315.74	0.09414	0.0084
$\nu_3+2\nu_4-2\nu_4$	E	A_1	2291.25	0.10855	0.0062
$\nu_3+2\nu_4-2\nu_4$	A_2	E	2301.19	0.09685	0.0048
$\nu_1+2\nu_4-2\nu_4$	E	E	2301.33	0.09601	0.0047
$2\nu_1-\nu_1$	A_1	A_1	2242.67	0.11496	0.0044

[a] Spectroscopic assignment of the vibrational band.
[b] Symmetry of the final vibrational state in $\boldsymbol{C}_{3v}(M)$.
[c] Symmetry of the initial vibrational state in $\boldsymbol{C}_{3v}(M)$.

of light in vacuum, k is the Boltzmann constant, $T = 300$ K, the Loschmidt constant $L = 2.68675 \times 10^{19}$ molecules cm^{-3} atm^{-1}, $T_0 = 273.15$ K. We obtained the value $Q_{vib} = 1.013457$ of the vibrational partition function at $T = 300$ K by summing over all variationally computed term values below 5000 cm^{-1}. It was shown in Ref. [32] that S_{vib} is a rather good approximation for the total integrated band intensity at a given temperature.

Only transitions with vibrational band intensities larger than 0.004 cm^{-2} atm^{-1} at $T = 300$ K are included in Tables 5 and 6, which also list the corresponding transition moments. Alternatively, we plot in Fig. 1 'effective' vibrational intensities that correspond to typical values for the integrated absorption coefficients of individual ro-vibrational transitions in the vibrational band in question. We define the effective intensity as

$$I_{fi} = S_{vib}(f \leftarrow i)/100. \quad (12)$$

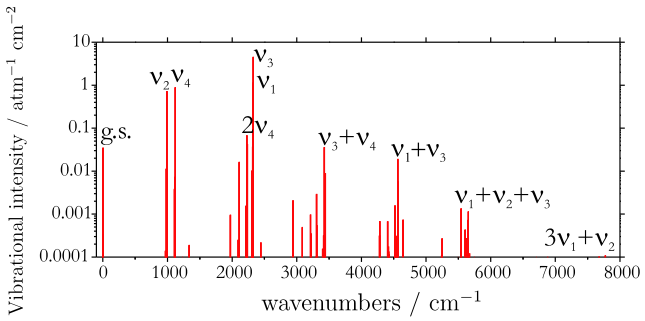

Fig. 1. Vibrational effective intensities of PH_3 computed at an absolute temperature of 300 K (note the logarithmic ordinate scale and see the text for details). Only transitions with an effective intensity larger than 0.004 cm^{-2} atm^{-1} are shown.

An approximate value for the integrated absorption coefficient of an individual ro-vibrational transition is obtained by multiplying $S_{\mathrm{vib}}(f \leftarrow i)$ in Eq. (11) by a Hönl-London factor times a rotational Boltzmann factor $\exp(-E_{\mathrm{rot}}/kT)/Q_{\mathrm{rot}}$ where E_{rot} is the rotational contribution to the energy of the lower state and Q_{rot} is the rotational partition function (see, for example, Section 12.3.1 of Ref. [26]). For the strongest ro-vibrational transitions in each of the bands considered here, we estimate this factor to be about 1/100 and this leads to Eq. (12).

5. Local-mode analysis of the PH_3 intensities

It can be seen in Tables 5 and 6 that there exist relations between the transition moments for transitions to excited stretching states. For example, the value of $\mu_{fi}(\nu_3)$ is approximately twice as large as that of $\mu_{fi}(\nu_1)$. We attribute this to the local-mode character of the stretching vibrations in PH_3 [10], and we make a detailed analysis here.

The local-mode behavior of the stretching modes in the PH_3 molecule can be determined geometrically and by analyzing the vibrational term values, the corresponding vibrational wavefunctions, and the vibrational transition moments. The normal-mode to local-mode transition with increasing vibrational excitation has already been extensively discussed (see, for example, Refs. [13,14]).

The bond angles of phosphine are close to 90° (for example, the AV(Q+d)Z+R PES that we use here has an equilibrium bond angle of $\alpha_e = 93.565°$) and, during the stretching vibration, the heavy P nucleus will remain largely stationary while the protons move. In consequence, the couplings between the individual-bond stretches are small and this leads to local-mode behavior.

At low energy, the vibrational spectrum is conveniently described in terms of the normal-mode model. However, as already mentioned, as the energy increases a normal-mode to local-mode transition takes place [13,14]. The Harmonically Coupled Anharmonic Oscillator (HCAO) model [13] explains the normal- to local-mode transition within the polyads of pure stretching states (i.e., the manifolds of stretching states with a common value of $n = n_1 + n_2 + n_3$, where these quantum numbers are defined in connection with Eq. (5)). In this model, the stretching vibration is taken to be that of identical anharmonic oscillators (one for each bond) with Morse potentials; these oscillators are coupled by one-body interactions expressed by harmonic creation and annihilation operators. The relationship between the parameters of the anharmonic oscillators and those of the coupling terms determines the normal-to-local transition.

Within a polyad, the states with lowest energy have the most pronounced local-mode properties while the states at the high-energy end can be 'normal' in character. This especially happens for molecules with significant anharmonic effects and small coupling between the stretching vibrations of the individual bonds. In the absence of this latter interaction, most stretching states will exhibit degeneracies, and when the interaction is small enough that the energy levels of the real molecule have such degeneracies, we say that they show local-mode behavior [13,14]. In Fig. 12 of Ref. [13] a normal- to local-mode correlation diagram for three equivalent anharmonic oscillators is presented. In Fig. 2 of the present work we show how, in accordance with the predictions from Fig. 12 of Ref. [13] (in which PH_3 is found at the right-hand, 'local-mode' edge), for the polyads with $n = 1, \ldots, 5$, the energy splitting between the lowest two states of each polyad decreases drastically as n increases. The energies plotted are those obtained with the AV(Q+d)Z+R PES. In Fig. 2, the normal-mode labeling of the lowest state of the polyad is given on the abscissa axis. Elementary local-mode theory predicts that this state should have the normal-mode label $n\nu_1$ and the local-mode label $(n,0,0)$ [13,14]. Fig. 2 shows, however, that for $n \geqslant 3$ we calculate the lowest state as $(n-1)\ \nu_1 + \nu_3$ with $n\nu_1$ slightly higher in energy. This 'energy reordering' and the increase of the energy splitting between $n = 2$ and $n = 3$ are caused by interaction with excited bending states. From Tables III and IV of Ref. [1] it is seen that near the $3\nu_1$ state (of A_1 symmetry) and the $2\nu_1 + \nu_3$ state (of E symmetry) there are several excited bending states that can interact with, and slightly shift, the $3\nu_1$ and $2\nu_1 + \nu_3$ states. Similar interactions take place for the $n = 4$ and 5 polyads.

Fig. 3 is a term level diagram showing the calculated energy-level patterns in the polyads with $n = 1, 2, 3, 4$. The energy levels in the figure exhibit the energy clustering predicted by local-mode theory [13,14]. In particular, within a given polyad the states at lowest energy form the 'tightest' clusters; these states exhibit a higher degree of local-mode behavior than the highest states in the polyad.

Apart from recognizing local-mode behavior in the energy-level patterns, we can also recognize it in the computed transition moments of PH_3. In local-mode theory, it is customary to approximate the dipole moment function by a function in the form [13]

$$\boldsymbol{\mu} = \mu_1(r_1)\ \mathbf{e}_1 + \mu_2(r_2)\ \mathbf{e}_2 + \mu_3(r_3)\ \mathbf{e}_3, \tag{13}$$

where $\mathbf{e}_i$, $i = 1, 2, 3$, is a unit vector pointing from the P nucleus towards proton i. In this approximation, the 'bond component' $\mu_i(r_i)\mathbf{e}_i$ describes the contribution to the dipole moment from the stretching of the individual bond P–H_i. Eq. (13) is highly analogous to the so-called Molecular-Bond (MB) representation of the dipole mo-

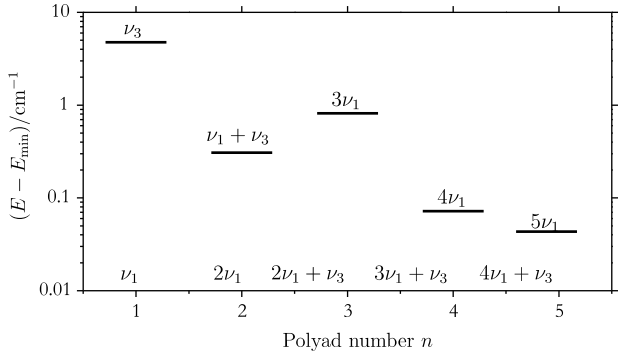

Fig. 2. The energy difference (in cm^{-1} on a logarithmic scale) between the two lowest states in the vibrational polyads of PH_3 with polyad number $n = 1$ through 5 (see text). The states are labeled by their normal-mode labels with that of the lowest state being given on the abscissa axis. The lowest states have the energies 2321.04, 4563.72, 6707.83, 8777.74, and 10757.10 cm^{-1} for the polyads n = 1, 2, 3, 4, and 5, respectively.

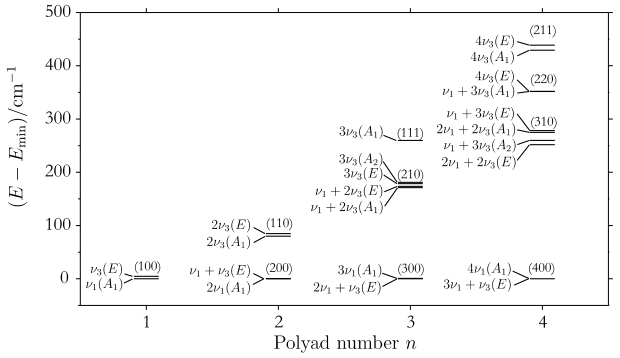

Fig. 3. Term value diagram for the $n \leqslant 4$ vibrational polyads of PH_3. The term values (in cm^{-1}) are plotted relative to the lowest state in each polyad. The states are labeled by their normal-mode labels and by the local-mode labels $(n_1 n_2 n_3)$. See also the caption of Fig. 2.

ment [9,30,33,34] that we employ in the intensity calculations of the present work (see Eq. (1) of Ref. [7]). However, while in each of the three equivalent 'bond components' $\mu_i(r_i)\mathbf{e}_i$ of Eq. (13), the function $\mu_i(r_i)$ depends on one bond length only, the analogous function $\bar{\mu}_i^{\text{Bond}}$ in Eq. (1) of Ref. [7] depends on all vibrational coordinates.

In connection with Eq. (5) we have defined the three quantum numbers n_1, n_2, n_3 to be those associated with the stretching of the individual bonds P–H_1, P–H_2, and P–H_3, respectively, and so the vibrational states have the local-mode labels [13,14] (n_1, n_2, n_3). Thus, we can approximate the vibrational transition moments μ_{fi} as

$$\begin{aligned}\langle n_1' n_2' n_3'|\boldsymbol{\mu}|n_1 n_2 n_3\rangle = {} & \langle n_1'|\mu_1|n_1\rangle \delta_{n_2',n_2}\delta_{n_3',n_3}\,\mathbf{e}_1 \\ & + \langle n_2'|\mu_2|n_2\rangle\ \delta_{n_1',n_1}\delta_{n_3',n_3}\,\mathbf{e}_2 \\ & + \langle n_3'|\mu_3|n_3\rangle\ \delta_{n_1',n_1}\delta_{n_2',n_2}\,\mathbf{e}_3, \end{aligned} \tag{14}$$

where $|n_1' n_2' n_3'\rangle = |n_1'\rangle|n_2'\rangle|n_3'\rangle$ is the vibrational wavefunction of the final state, and $|n_1 n_2 n_3\rangle = |n_1\rangle|n_2\rangle|n_3\rangle$ is that of the initial state. When $n_1' = n_2' = n_3'$ and $n_1 = n_2 = n_3$, by symmetry, the matrix elements of the vibrational basis functions are equal:

$$\langle n_1'|\mu_1|n_1\rangle = \langle n_2'|\mu_2|n_2\rangle = \langle n_3'|\mu_3|n_3\rangle. \tag{15}$$

We can now investigate to which extent the vibrational transition moments in Table 5 satisfy the relations imposed by local-mode theory. We consider vibrational transitions starting in the vibrational ground state. For the transitions to the first polyad of states with $n_1 + n_2 + n_3 = 1$, the transition moments are

$$\begin{aligned} |\langle 0|\boldsymbol{\mu}|\nu_1\rangle| &= |\langle 0|\mu_1|1\rangle|\sqrt{1+\frac{2}{3}(\cos\alpha_{12}+\cos\alpha_{13}+\cos\alpha_{23})} \\ |\langle 0|\boldsymbol{\mu}|\nu_{3a}\rangle| &= |\langle 0|\mu_1|1\rangle|\sqrt{1-\frac{2}{3}\left(\cos\alpha_{12}+\cos\alpha_{13}+\frac{1}{2}\cos\alpha_{23}\right)} \\ |\langle 0|\boldsymbol{\mu}|\nu_{3b}\rangle| &= |\langle 0|\mu_1|1\rangle|\sqrt{1-\cos\alpha_{23}} \end{aligned} \tag{16}$$

where in the tradition of local-mode theory, we consider stretching motion only and take the bond angles α_{ij} to be constants.

For PH_3, we approximate $\alpha_{12} = \alpha_{13} = \alpha_{23} = 90^\circ$ and so Eq. (16) yields

$$|\langle 0|\boldsymbol{\mu}|\nu_1\rangle| = |\langle 0|\boldsymbol{\mu}|\nu_{3a}\rangle| = \langle 0|\boldsymbol{\mu}|\nu_{3b}\rangle| = |\langle 0|\mu_1|1\rangle|. \tag{17}$$

According to Table 5, $|\langle 0|\boldsymbol{\mu}|\nu_1\rangle| = 0.06956$ D. We obtain the transition moment for the ν_3 band from Eq. (17) by adding the transition moments corresponding to the two components of this transition:

$$|\langle 0|\boldsymbol{\mu}|\nu_3\rangle| = 2|\langle 0|\boldsymbol{\mu}|\nu_1\rangle| = 2|\langle 0|\mu_1|1\rangle| = 0.13912\ \text{D}; \tag{18}$$

this value is close to the computed value of 0.13789 D from Table 5.

For the transitions to the second polyad of states with $n_1 + n_2 + n_3 = 2$, we obtain approximate transition moments as

$$\begin{aligned} |\langle 0|\boldsymbol{\mu}|200;A_1\rangle| &= |\langle 0|\mu_1|2\rangle|\sqrt{1+\frac{2}{3}(\cos\alpha_{12}+\cos\alpha_{13}+\cos\alpha_{23})}, \\ |\langle 0|\boldsymbol{\mu}|200;E_a\rangle| &= \langle 0|\mu_1|2\rangle\sqrt{1-\frac{2}{3}\left(\cos\alpha_{12}+\cos\alpha_{13}+\frac{1}{2}\cos\alpha_{23}\right)}, \\ |\langle 0|\boldsymbol{\mu}|200;E_b\rangle| &= \langle 0|\mu_1|2\rangle\sqrt{1-\cos\alpha_{23}}. \end{aligned} \tag{19}$$

With $\alpha_{ij} = 90^\circ$ these transition moments become equal

$$|\langle 0|\boldsymbol{\mu}|200;A_1\rangle| = |\langle 0|\boldsymbol{\mu}|200;E_a\rangle| = |\langle 0|\boldsymbol{\mu}|200;E_b\rangle| = |\langle 0|\mu_1|2\rangle| \tag{20}$$

and we can equate them with the transition moment of the $2\nu_1$ band which, from Table 5, has the value 0.00351 D. We now have

$$|\langle 0|\boldsymbol{\mu}|\nu_1+\nu_3\rangle| = |\langle 0|\boldsymbol{\mu}|200;E\rangle| = 2|\langle 0|\mu_1|2\rangle| = 0.00702\ \text{D}, \tag{21}$$

which is close to the value of 0.00641 D from Table 5.

We have seen that for the first and second polyads (consisting of states with $n = n_1 + n_2 + n_3 = 1$ and 2, respectively), the computed transition moments from Table 5 satisfy well the relations imposed by local-mode theory. For polyads at higher energy, the agreement with the results of local-mode theory deteriorates. The local-mode theory assumes that the molecule has stretching states only, no bending states. The transitions from the vibrational ground state to the high-energy stretching states are very weak, and the very small transition moments are easily changed by weak interactions with excited bending states. Also, the terms neglected in the rather simple dipole moment function of Eq. (13) (which describe interactions between the stretches of individual bonds) are expected to play increasingly important roles at high energy where the stretching amplitudes are large.

It follows from Eqs. (17) and (20), in conjunction with Table 5, that the ratio $|\langle 0|\mu_1|2\rangle|/|\langle 0|\mu_1|1\rangle| \approx 0.05$. Obviously, if we take $\mu_i(r_i) = Cr_i$ (that is, $\mu_i(r_i)$ to be proportional to r_i), this ratio would be zero in the harmonic approximation. The value of 0.05 is, however, similar to the value of 0.11 obtained for $\mu_i(r_i) = Cr_i$ when we take the $|n_i\rangle$ to be Morse-oscillator eigenfunctions. Possibly we could obtain a better agreement between the two ratios if we used a more realistic dipole moment function, for example $\mu_i(r_i) = C' r_i \exp(-br_i)$, where C' and b are constants.

6. Summary and conclusion

In the present work, we have extended and complemented recent calculations of the vibrational term values [1] and transition moments [7] for the PH_3 molecule in its electronic ground state. The starting point for the new calculations is the AV(Q+d)Z+R PES obtained in Ref. [1] and the ATZfc DMS from Ref. [7]. The previous calculation of vibrational transition moments [7] was based on an earlier PES, obtained by refining an *ab initio* surface by Wang et al. [10] in least-squares fittings to experimental data, and on the ATZfc DMS also used in the present work. We have extended our previous calculations of vibrational transition moments in that we now consider all vibrational transitions with significant intensities below 7000 cm^{-1}; in our previous calculation we only considered a smaller number of selected transitions. We further demonstrate here that the theoretical intensity results of the present work are in accordance with the predictions of local-mode theory.

We noted in connection with Table 4 that the relative root-mean-square deviation σ_{rel} [Eq. (10)] between the experimentally derived transition-moment values in Table 4 and the theoretical values from Ref. [7] is 0.39, whereas the analogous deviation between the experimental values and the theoretical values from the present work is 0.14. This substantial improvement is, of course, to a large extent caused by the large improvements for the weak transitions to the $2\nu_4^0$ and $2\nu_4^2$ states (see Table 4). The value of $\sigma_{\text{rel}} = 0.14$ suggests, however, that we can theoretically reproduce experimental vibrational transition-moment values with relative deviations on the order of magnitude of 10%. We find this very encouraging as the accuracies achieved in typical experimental determinations of such transition moments are hardly better. Thus, we are approaching a situation where theoretical calculations of intensity information can compete with, and possibly in some cases replace, experimental determinations, at least for small molecules.

Relative to the vibrational transition-moment calculations of Ref. [7] we have obviously improved the PES, but not the DMS. It is remarkable that the new PES produces such a substantial

improvement of the description of weak band intensities. It suggests that the wavefunctions of the highly excited states involved in the weak bands, and thus the corresponding vibrational transition moments, are crucially dependent on the shape of the PES.

Acknowledgments

Part of this work was carried out while S.N.Y. and P.J. were visiting scientists, in the framework of the MEC research program FINURA (financed by the Spanish Government through contract No. FPA2007-63074), at the Departamento de Física Aplicada, Facultad de Ciencias Experimentales of the Universidad de Huelva. They are extremely grateful for the kind hospitality extended to them and for financial support. We acknowledge support from the European Commission through contract No. MRTN-CT-2004-512202 "Quantitative Spectroscopy for Atmospheric and Astrophysical Research" (QUASAAR). The work of P.J. is supported in part by the Fonds der Chemischen Industrie and that of S.N.Y. by the Deutsche Forschungsgemeinschaft. R.I.O. is grateful for partial support from the RFBR Grant No. 06-02-16082-a. The work of M.C. is supported in part by Junta de Andalucía (Spain) through contract No. P07-FQM-03014.

References

[1] R.I. Ovsyannikov, W. Thiel, S.N. Yurchenko, M. Carvajal, P. Jensen, J. Chem. Phys. 129 (2008) 044309/1-8.
[2] S.N. Yurchenko, W. Thiel, P. Jensen, J. Mol. Spectrosc. 245 (2007) 126–140.
[3] G.A. Petersson, A. Bennett, T.G. Tensfeldt, M.A. Al-Laham, W.A. Shirley, J. Mantzaris, J. Chem. Phys. 89 (1988) 2193–2218.
[4] G.A. Petersson, M.A. Al-Laham, J. Chem. Phys. 94 (1991) 6081–6090.
[5] S.N. Yurchenko, M. Carvajal, P. Jensen, F. Herregodts, T.R. Huet, Chem. Phys. 290 (2003) 59–67.
[6] S.N. Yurchenko, W. Thiel, S. Patchkovskii, P. Jensen, Phys. Chem. Chem. Phys. 7 (2005) 573–582.
[7] S.N. Yurchenko, M. Carvajal, W. Thiel, P. Jensen, J. Mol. Spectrosc. 239 (2006) 71–87.
[8] S.N. Yurchenko, M. Carvajal, P. Jensen, H. Lin, J.J. Zheng, W. Thiel, Mol. Phys. 103 (2005) 359–378.
[9] S.N. Yurchenko, W. Thiel, M. Carvajal, H. Lin, P. Jensen, Adv. Quant. Chem. 48 (2005) 209–238.
[10] D. Wang, Q. Shi, Q.-S. Zhu, J. Chem. Phys. 112 (2000) 9624–9631.
[11] P. Jensen, G. Osmann, I.N. Kozin, in: D. Papoušek (Ed.), Vibration–Rotational Spectroscopy and Molecular Dynamics, World Scientific, Singapore, 1997.
[12] P.R. Bunker, P. Jensen, Molecular Symmetry and Spectroscopy, second ed., NRC Research Press, Ottawa, 1998.
[13] M.S. Child, L. Halonen, Adv. Chem. Phys. 57 (1984) 1–58.
[14] P. Jensen, Mol. Phys. 98 (2000) 1253–1285.
[15] MOLPRO, version 2002.3 and 2002.6, a package of *ab initio* programs written by H.-J. Werner and P.J. Knowles, with contributions from R.D. Amos, A. Bernhardsson, A. Berning, et al.
[16] C. Hampel, K. Peterson, H.-J. Werner, Chem. Phys. Lett. 190 (1992) 1–12. and references therein; The program to compute the perturbative triples corrections has been developed by M.J.O. Deegan, P.J. Knowles, Chem. Phys. Lett. 227 (1994) 321–326.
[17] G.D. Purvis, R.J. Bartlett, J. Chem. Phys. 76 (1982) 1910–1918.
[18] M. Urban, J. Noga, S.J. Cole, R.J. Bartlett, J. Chem. Phys. 83 (1985) 4041–4046.
[19] K. Raghavachari, G.W. Trucks, J.A. Pople, M. Head-Gordon, Chem. Phys. Lett. 157 (1989) 479–483.
[20] T.H. Dunning, J. Chem. Phys. 90 (1989) 1007–1023.
[21] D.E. Woon, T.H. Dunning, J. Chem. Phys. 98 (1993) 1358–1371.
[22] R.A. Kendall, T.H. Dunning, R.J. Harrison, J. Chem. Phys. 96 (1992) 6796–6806.
[23] A.K. Wilson, T.H. Dunning, J. Chem. Phys. 119 (2003) 11712–11714.
[24] D.A. Helms, W. Gordy, J. Mol. Spectrosc. 66 (1977) 206–218.
[25] K. Kijima, T. Tanaka, J. Mol. Spectrosc. 89 (1981) 62–75.
[26] P.R. Bunker, P. Jensen, Fundamentals of Molecular Symmetry, IOP Publishing, Bristol, 2004.
[27] V. Špirko, P. Jensen, P.R. Bunker, A. Čejchan, J. Mol. Spectrosc. 112 (1985) 183–202.
[28] G. Tarrago, N. Lacome, A. Lèvy, G. Guelachvili, B. Bèzard, P. Drossart, J. Mol. Spectrosc. 154 (1992) 30–42.
[29] O.N. Ulenikov, E.S. Bekhtereva, V.A. Kozinskaia, J.J. Zheng, S.-G. He, S.-M. Hu, Q.-S. Zhu, C. Leroy, L. Pluchart, J. Mol. Spectrosc. 215 (2002) 295–308.
[30] S.N. Yurchenko, M. Carvajal, H. Lin, J.J. Zheng, W. Thiel, P. Jensen, J. Chem. Phys. 122 (2005) 104317.
[31] S.N. Yurchenko, W. Thiel, M. Carvajal, P. Jensen, Chem. Phys. 346 (2008) 146–159.
[32] C. Cottaz, G. Tarrago, I. Kleiner, L.R. Brown, J. Mol. Spectrosc. 209 (2001) 30–49.
[33] S.-G. He, J.J. Zheng, S.-M. Hu, H. Lin, Y. Ding, X.-H. Wang, Q.-S. Zhu, J. Chem. Phys. 114 (2001) 7018–7026.
[34] R. Marquardt, M. Quack, I. Thanopulos, D. Luckhaus, J. Chem. Phys. 119 (2003) 10724–10732.